

Assessing Tidal Current Velocity Across Different Water Depth Layers in Khenifiss Lagoon (Southern Atlantic Coast of Morocco) – Implications for Potential Tidal Energy Extraction

Hamza El Behja^{1*}, Abdelmounim El M'rini¹, Zouhayr El-Wamdeni²,
Mohammed Bouchkara³, Driss Nachite¹, Khalid El Khalidi³,
Hichame El-Hassani⁴, Bendahhou Zourarah³

¹ Research Laboratory in applied and marine Geosciences, Geotechnics and Geohazards (LR3G), Faculty of Sciences, Abdelmalek Essaâdi University, 93000, Tetouan, Morocco

² Environmental Geology and Natural Resources Laboratory, Faculty of Sciences, Abdelmalek Essaâdi University, 93000, Tetouan, Morocco

³ Marine Geosciences and Soil Sciences Laboratory (URAC 45), Department of Earth Sciences, Faculty of Sciences, Chouaïb Doukkali University, El Jadida, Morocco

⁴ Applied Geosciences and Geological Engineering, Faculty of Sciences and Technology of AL-Hoceima, Abdelmalek Essaâdi University, 93000, Tetouan, Morocco

* Corresponding author's e-mail: hamza.elbehja@etu.uae.ac.ma

ABSTRACT

The global industrial economy is heavily reliant on fossil fuels, but their depletion and environmental impact require a rapid shift to low-carbon energy sources. Coastal lagoons offer a potential sustainable energy source through the extraction of energy from tidal currents at different water depths. Therefore, the measurement of currents in each depth layer is crucial for determining suitable locations and studying the feasibility of harnessing this renewable energy through tidal power generation technologies. This study focuses on evaluating the potential of tidal currents for generating marine renewable energy in the Khenifiss Lagoon, a protected area in southern Morocco, for local use, with the goal of supporting the sustainability of this ecosystem. The lagoon's hydrodynamics are primarily dominated by tides, with the semi-diurnal component (M_2) dominating the tidal cycle (period of 12 h 25) with 1.5 to 3.2 m of tidal range. The Multicell Argonaut-XR ADCP is employed to measure current velocities over two days at two specific stations within the lagoon without the intention of establishing a comparative analysis between them. Station 1 has 1 m intervals across an 8 m depth, and Station 2 has 0.5 m intervals across a 5 m depth. The results reveal that at Station 1, layers 2, 3, 4, and 5 (-2 to -5 m depth) exhibited consistent current velocity conditions, making them well-suited for power density conversion. The average power density range in these layers ranged from 54.926 W/m² to 65.223 W/m². Similarly, at Station 2, layers 2, 3, 4, 5, and 6 (-2.5 to -4.5 m depth) displayed favorable current velocity conditions for power density conversion, with an average power density range of 23.911 W/m² to 36.630 W/m². This work establishes a foundation for more detailed tidal current resource assessments for future tidal energy development in the Khenifiss lagoon and such a semi-enclosed natural system.

Keywords: tidal energy, marine renewable energy, ADCP, power density, costal environment, costal lagoon.

INTRODUCTION

The global industrial economy is still heavily reliant on fossil fuels as its primary energy source (Musa et al., 2018). However, as global oil

and gas reserves are projected to be depleted by mid-century (Musa et al., 2018), this reliance is becoming increasingly problematic, posing a significant threat to supply security (Bahadori et al., 2013). Furthermore, the environmental impact of

fossil fuels is a major and growing concern (Musa et al., 2018). The pressing challenges posed by fossil fuels, encompassing environmental, climate, and economic dimensions, emphasize the urgent need for a rapid transition to low-carbon energy systems, particularly renewables. The pressing challenges posed by fossil fuels, encompassing environmental, climate, and economic dimensions, emphasize the urgent need for a rapid transition to low-carbon energy systems, particularly renewable. The adoption of renewable energy technologies, however, is hampered by a variety of constraints, including economic, socio-cultural, and institutional factors (Vanegas Cantarero, 2020). In Morocco, the National Energy Strategy of 2009 envisaged putting the country on the pathway for a real energy transition, with plans to implement solar, wind, and hydroelectric projects and aim to achieve a target of 52% of total installed electrical power from renewable energy sources by 2030 (IEA, 2019), emerging as a regional energy hub and a driving force behind the clean energy transition throughout the African continent (IEA, 2019).

The vast ocean, which covers 71% of the Earth's surface, has enormous energy potential (Wang et al., 2019). Offshore wind, offshore solar, tidal range, marine current, wave, salinity gradient, and ocean thermal are among the sources used to generate marine renewable energy (Elabban et al., 2014; Multon, 2013). Tidal energy, which is generated by the moon's and sun's gravitational forces on Earth's waters as well as the planet's rotation, has the advantage of predictability over solar and wind energy, and it can be expressed as either the potential energy of the water level difference during the ebb and flood or the kinetic energy of a tidal current (Zabihian and Fung, 2011). Marine current energy offers a clean and sustainable way to generate electricity with little negative environmental effects (Dal Ferro, 2006; Rourke et al., 2010). Assessing marine current energy necessitates careful consideration of current velocity characteristics and fluctuations, which must be measured and analyzed to determine the feasibility of implementing marine current energy devices for energy extraction at potential sites (Boyle, 1996; Dubi, 2007). Moreover, the placement of tidal stream turbines at the appropriate depth is carefully considered to improve efficiency and optimization (Siagian et al., 2019b). Failure to calculate the vertical current profile accurately can result in non-optimal power

density, resulting in incorrect positioning of tidal turbine devices (Siagian et al., 2019b). Therefore, it is crucial to comprehend the distribution of tidal current velocities when evaluating the viability of a site for tidal energy extraction. This understanding allows for the selection of an appropriate location and depth to implement a recovery system.

Tidal streams refer to areas where tidal flows are concentrated, presenting a substantial energy source (Neill et al., 2021). Hydrokinetic turbines, similar to those used in wind energy, can harness the kinetic energy from these tidal streams, offering significant potential for power generation (Neill et al., 2021), and the tidal stream energy industry is currently in the nascent phase of its development (Maxim et al., 2009). The methodology used in this study to estimate the power density at different depth layers of water, as measured by the ADCP (acoustic doppler current profiler), has been applied in numerous locations worldwide. The study of Siagian et al. (2019b), conducted in the East Flores Waters in Indonesia, assessed marine current energy by analyzing current velocity characteristics and fluctuations across different depth layers. The findings revealed two specific depth layers, namely -3.5 to -5.5 meters from the Lowest Astronomical Tide (LAT) and -7.5 to -9.5 meters from the LAT, which exhibited highly promising potential energy. These layers exhibited the highest speeds of tidal currents, measuring 3.69 m/s and 3.68 m/s, respectively. Furthermore, the study indicated that the bottom layer had a lower energy capacity, suggesting that this site is suitable for the installation of seabed-mounted tidal turbines. In a study conducted by Maxim et al. (2009), a combination of High-Frequency Radars (HFR) for remotely sensing surface velocities and ADCP velocity profiles was employed to assess hydrokinetic resources at a near-shore site in the Iroise Sea. This approach enabled the evaluation of tidal current variability and power density variations in three dimensions. The analysis revealed two regions characterized by substantial energy potential. Guerra et al. (2017) conducted a study in the Chacao Channel, an energetic tidal channel situated in the northernmost part of Chile. The study utilized both ADCP measurements and numerical modeling techniques. The results obtained were used to estimate the kinetic power density of the tidal currents in the Chacao Channel, which have a mean kinetic power density above 5 KW/m² more than 20% of the time. The Oualidia Lagoon in Morocco was the focus

of a study by Bouchkara et al. (2023) aimed at estimating the potential energy power derived from tidal currents. The study utilized the ADCP to measure current velocities at three different stations, enabling the investigation of tidal patterns across various depths. The study findings indicated that at station 1, the layer located at a depth of 3.5 meters, the power density value was measured at 235.344 W/m². Likewise, at station 2, at the same depth, the power density value was recorded as 32.86 W/m². At a depth of 3 meters, station 3 exhibited a power density value of 75.157 W/m². These measurements highlight the potential utilization of current velocities as a renewable energy source in the lagoon's main channel.

The main objective of this study is to assess the current velocity at various water depth layers within the tidal stream channel of Khenifiss Lagoon. Additionally, it seeks to evaluate the potential energy of tidal currents in terms of power density at two specific locations within the main channel of this coastal lagoon, without the intention of establishing a comparative analysis between them. The obtained results might be employed to evaluate the feasibility of generating electricity from current energy in the lagoon and to determine the optimal depth layer for implementing marine current energy devices. This is particularly relevant for the private sector, which plans to develop tourist projects while upholding ecological integrity, given the lagoon's protected status. In addition to solar panels and wind turbines, this knowledge contributes to ecosystem preservation and sustainable development by guiding decision-makers to prioritize informed choices that balance environmental conservation with the drive toward a sustainable future.

STUDY AREA

Located in the coastal Sahara, south of Morocco, Khenifiss Lagoon (known as Naila Lagoon to the locals) is the biggest lagoon and the most important wetland in the Atlantic Moroccan desert (Amimi et al., 2021). The lagoon is a 65 Km² body of water that belongs to the national park of Khenifiss, which has been a protected area since 2006. It extends over 20 kilometers into the Moghrebian limestone-sandstone plateau (Elbelrhiti et al., 2008), eventually leading to a vast salt flat called "Sebkha de Tazra" (Lakhdar et al., 2004). On its eastern and southern sides, the lagoon is surrounded by a cliff measuring 25–35 meters in height,

while the western coast is characterized by active dunes (Mirari et al., 2020). These dunes contribute to the siltation phenomenon experienced by the lagoon, which in turn affects the extent of its water body (El Behja et al., 2024a; 2024c)

The entrance, also known as Fom Agoutir, is located at approximately 12°13'33" W longitude and 28°02'28" N latitude (Beaubrun, 1976). It allows the lagoon to communicate with the Atlantic Ocean, reaching depths of 5 to 6 meters and cutting through the dune cord along the coast (Beaubrun, 1976). The channel, which extends over a length of 20 kilometers, can be subdivided into three sections: The upper section, a narrow channel-oriented ENE-WSW, is 7 kilometers long and has depths ranging from 6 to 15 meters (Beaubrun, 1976). The current in this section is generally strong, sometimes exceeding 1 m/s, leading to the formation of coarse sediment (Lakhdar et al., 2004). The middle section, oriented NNW-SSE, is 4 kilometers long and straight, and the seabed consists of sandy substrates with a depth varying between 3 and 4 meters (Beaubrun, 1976). In this zone, the current is relatively lower compared to the upper section (Lakhdar et al., 2004). The lower section, oriented ENE-WSW and extending for 9 kilometers, runs parallel to the upper section. It has a depth ranging from 5 meters in its eastern part to 0.20 meters and is covered in sand (Beaubrun, 1976). This zone is characterized by a very slight oceanic influence compared to the preceding sections (Lakhdar et al., 2004).

The semi-diurnal component (M_2) of the current dominates the tidal cycle in Khenifiss Lagoon, with a period of 12 hours and 25 minutes (Lakhdar et al., 2004). The ebb and flow rhythm controls the hydrodynamics within the lagoon, which is characterized by an alternating and bidirectional water circulation pattern (Lakhdar et al., 2004; El Behja et al., 2024b). The tidal range varies within the Khenifiss Lagoon, measuring 3.20 meters at the entrance, 3.00 meters in the central zone (12 kilometers from the inlet), and 1.50 meters in the upstream zone (20 kilometers from the inlet) (Beaubrun, 1976).

MATERIAL AND METHOD

Velocity measurement

The SonTek Argonaut-XR Acoustic Doppler Current Profiler (ADCP) was used as a measurement instrument in two specific locations within

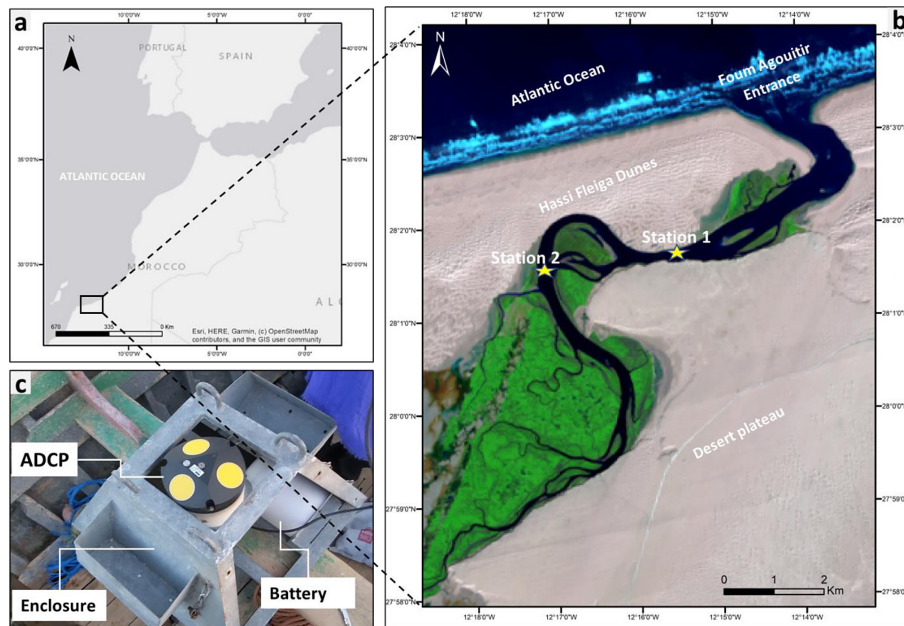


Figure 1. (a) Geographic location of the study area; (b) top view of Khenifiss lagoon and the location of measured stations (Station 1 and Station 2); (c) photo shows the SonTek Argonaut-XR ADCP instrument arrangement before deployment

the Khenifiss lagoon's main channel. Figure 1c depicts the ADCP arrangement, which is securely placed inside an enclosure to ensure its stability and functionality during deployment. The device operated at a frequency of 1.5 MHz, and it was positioned 0.5 meters above the seabed. For station 1, it comprised 8 layers of current measurement in all directions, while for station 2, it had 10 layers. The data collected from both stations was used to create vertical velocity profiles. These profiles spanned the period from February 4, 2022, to February 8, 2022, providing valuable insights into the vertical flow dynamics within the lagoon. As illustrated in Figure 2, velocity was measured at every 1-meter layer (8-depth layer) at station 1, where layer 8 is closest to the water's surface while layer 1 is directly above the ADCP, and every 0.5-meter layer (8-depth layer) at station 2, where layer 10 is closest to the water's surface while layer 1 is directly above the ADCP. Table 1 shows the configuration of measuring stations. The deployment depth in Station 1 was approximately 9m and 6m in Station 2. The velocity was recorded every 600 seconds at each station. The current characterization entails determining the maximum, and average velocity for each depth layer. The mean velocity is the average of the current velocity magnitudes over the measuring period (2 days for each station), and the maximum sustained velocity is the maximum current

observed. Figure 3 shows the water level conditions at the lagoon's entrance during the measurement period. The measurements were conducted between the spring and neap tides, capturing the transitional phase between these two tidal states.

Power density estimation

The generation of power density from marine currents entails using a variety of technologies, such as turbines, to transform the kinetic energy of ocean currents into electrical power (Ghefiri et al., 2018; Rourke et al., 2010). Similar concepts underlie wind energy and the use of current speed as a source of power density (Rourke et al., 2009). However, compared to similarly sized wind energy devices operating at comparable velocities, seawater has a higher density, which results in greater power output (Bryden et al., 2004; Hwang et al., 2009). For example, tidal currents produce power densities between 500 and 1.000 W/m² at flow rates between 1 and 1.3 m/s (Hagerman and Polagye, 2006). Given that air has a lower density than water; wind turbines need wind speeds of 9.3 to 11.8 m/s to produce equivalent power densities (Hagerman and Polagye, 2006). The power density that can be generated from marine currents is directly proportional to the current velocity parameter; it rises quite quickly with current speed (Hagerman and Polagye, 2006). The theoretical

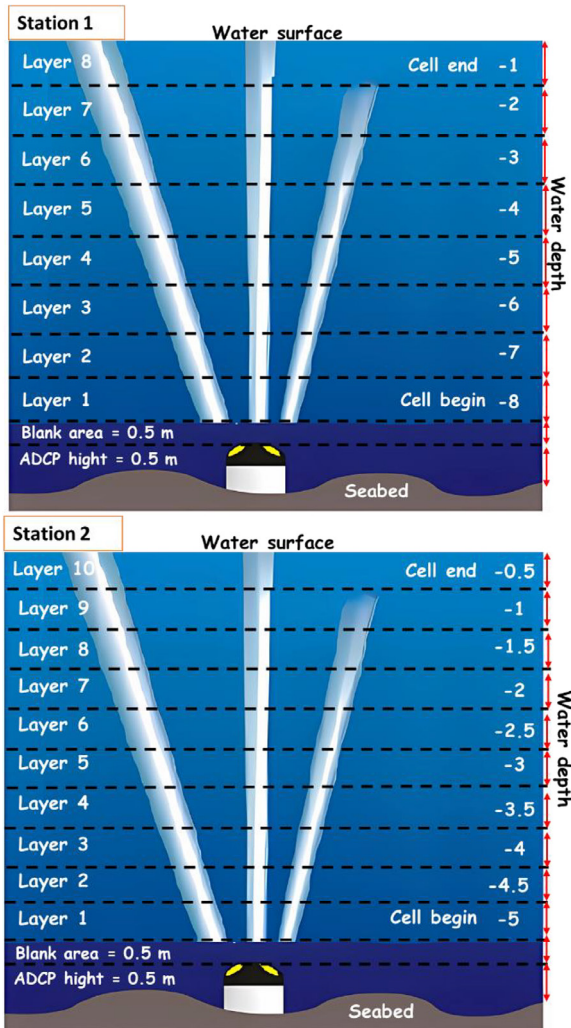


Figure 2. ADCP depth layer profile; Station 1: velocities were recorded at every 1m layer (eight-layer depth); layer 8 is closest to the water’s surface, whereas layer 1 (-8 m) is directly above the ADCP; Station 2: velocities were recorded at every 0.5m layer (ten-layer depth); layer 10 is closest to the water’s surface, whereas layer 1 (-5 m) is directly above the ADCP

power potential for an individual turbine is calculated as the cube of the free stream velocity (Guerra et al., 2017; Neill et al., 2021).

$$P = \frac{1}{2} \rho(u)^3 \tag{1}$$

where: P is power density per unit area intercepted by the device (in watts per square meter), u is the flow speed (in meters per second), and ρ density of seawater (1025 kg/m^3).

Considering the efficiency of a specific turbine and the turbine’s swept area, Equation 1 can be modified by multiplying it by the power coefficient C and the swept area of the turbine A , as shown in Equation 2 (Neill et al., 2021).

$$P = \frac{1}{2} \rho C(u)^3 A \tag{2}$$

In our study, we focused on directly measuring the amount of energy that can be converted into power density from tidal currents at each depth layer in two locations (Station 1 and Station 2), and therefore, we did not take into account the efficiency of the turbine (Siagian et al., 2019b). Also, it should be noted that small variations in quantity can lead to significant changes in available power density because power is a function of the cube of velocity (González-Gorbeña et al., 2015).

RESULT AND DISCUSSION

Analysis of vertical current velocity distribution

A comprehensive understanding of the geographical distribution of marine current velocities is crucial for the effective implementation

Table 1. Configuration of measuring stations

Instrument	ADCP SonTek Argonaut-XR frequency, 1.5 Mhz set,	
	Station 1	Station 2
Station No.	28.04178144 (°N) 12.22923156 (°E)	28.02461512(°N) 12.28568026 (°E)
Location	04/02/2022 – 06/02/2022	06/02/2022 – 08/02/2022
Deployment date	2 x 24	2 x 24
Duration (hours)	9	6
Deployment depth (m)	8.5	5.5
Depth measurement (m)	1	0.5
Vertical layer size/bin (m)	8	10
Total layers	600	600
Interval time sampling (s)	0.5	0.5
Blank area (m)		

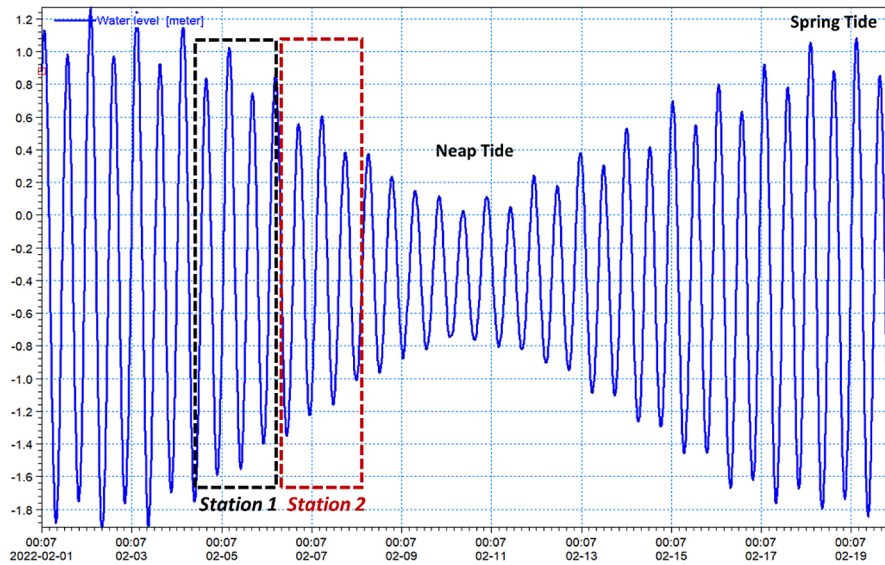


Figure 3. Water level conditions at the entrance of the lagoon during the period of measurements, based on data from the Biscary Irish Monitoring and Forecasting Centre (IBI-MFC) (<https://marine.copernicus.eu/about/producers/ibi-mfc>)

of marine current energy devices (Rourke et al., 2010). Based on the results represented in Figure 4, when comparing layers at each ADCP location, no clear velocity stratification is observed. Nevertheless, the main channel of the

Khenifiss lagoon displays alternating currents associated with semi-diurnal tidal patterns (El Behja et al., 2024b; Lakhdar Idrissi et al., 2004). Since turbine installations are generally more effective in regions where tidal currents

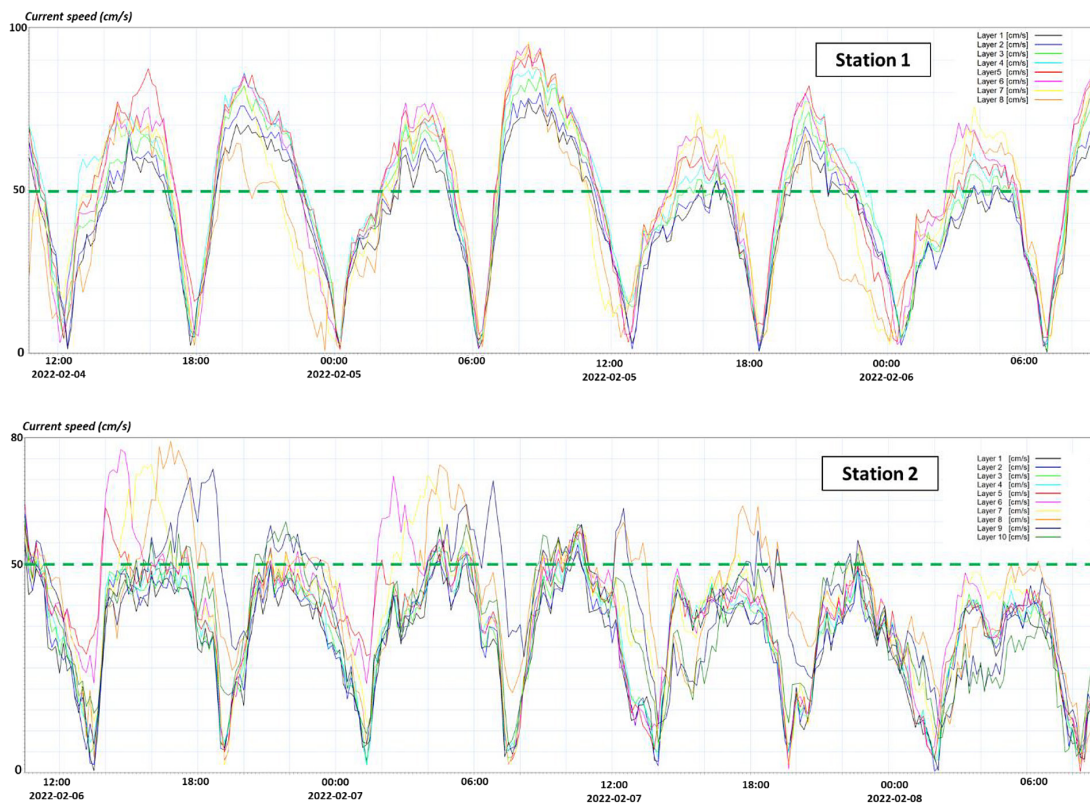


Figure 4. Variations in current speed across different layers at Stations 1 and 2. The green dashed line indicates the cut-in speed at 0.5 m/s (velocity below cut-in speed, rotor cannot turn power train, means electric power = 0; Velocity above cut-in speed means electric power = fluid power x power train efficiency)

consistently reverse along a specific axial direction (González-Gorbeña et al., 2015), the presence of these alternating currents suggests that the Khenifiss lagoon could be suitable for such installations. The results of the current velocity distribution at each station are inspected and analyzed. We followed the approach taken by Siagian et al. (2021), and we employed a vertical presentation of current velocities to detect variations across different depths. A vertical graph was presented below the LAT value to illustrate significant water changes (Pu et al., 2017; Siagian et al., 2019b). The vertical profiling of current velocity, represented in Figure 5, aided in identifying the layer with potential for

further investigation in harnessing current energy (Bouchkara et al., 2023; Siagian et al., 2021).

Current measurement results, represented in Figure 5 and illustrated in Table 2, indicate a maximum speed of 95.6 cm/s at layer 2 (-7 m depth), with an average speed of 47.5 cm/s at Station 1. At Station 2, the maximum speed value was recorded at layer 3 (-4 m depth), which was 79.2 cm/s, while the average speed was 41.5 cm/s. The maximum current velocity at the bottom layer successively at stations 1 and 2 is 94.2 cm/s and 60.0 cm/s, while the average current velocity is successively 43.1 cm/s and 35.5 cm/s. Drawing insights from Figure 3, velocity measurements at Station 1 were taken in proximity to the spring tide, whereas those at

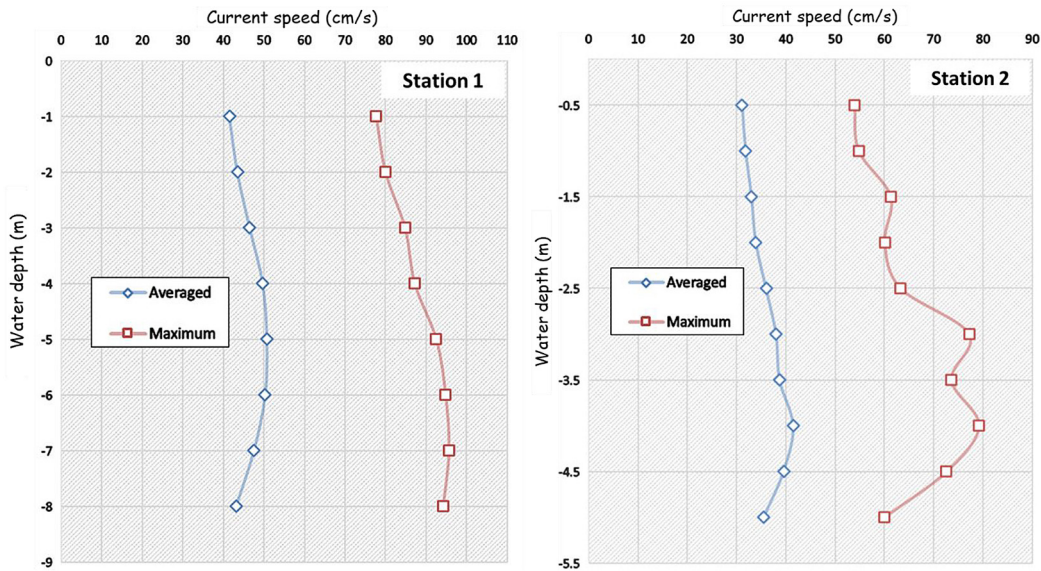


Figure 5. Averaged current velocity profile derived from ADCP stations (Station 1 and Station 2). The upper layer situated below the LAT

Table 2. Current velocity profiles measured by ADCP in each station (depth layer profile, minimum, average, and maximum velocity)

Depth layer profile no.	Station 1			Station 2		
	Water depth layer (meters)	Current speed (cm/s)		Water depth layer (meters)	Current speed (cm/s)	
		Average	Maximum		Average	Maximum
10	-	-	-	-0.5	31.1	54.0
9	-	-	-	-1	31.8	54.8
8	-1	41.5	77.7	-1.5	33.0	61.3
7	-2	43.5	80.0	-2	33.9	60.1
6	-3	46.5	84.8	-2.5	36.0	63.3
5	-4	49.6	87.2	-3	38.0	77.2
4	-5	50.7	92.5	-3.5	38.7	73.6
3	-6	50.3	94.8	-4	41.5	79.2
2	-7	47.5	95.6	-4.5	39.6	72.6
1	-8	43.1	94.2	-5	35.5	60.0

Station 2 were conducted closer to the neap tide. It's essential to note that this temporal distinction significantly influences the observed results.

There is no clear distribution trend in the vertical current velocity profiles, the average current speed appears to be higher in the middle layers than in the bottom and surface layers at both stations. Layers 2–6 at Station 1 have the highest values (ranging from 46.5 cm/s to 50.7 cm/s), and the same layers at Station 2 have the highest values (ranging from 36 cm/s to 41.5 cm/s).

During the measurement, both Station 1 and Station 2 exhibit a noticeable pattern, displaying sinusoidal behavior that follows the tides (El-Geziry and Couch, 2009; Wei et al., 2016). Figure 4 demonstrates the available current capacity,

which can be converted into power density at each layer. When the current velocity falls below the cut-in speed, the turbine remains motionless and produces no power. When the current velocity exceeds the turbine's rated speed, the power output remains constant. By utilizing a cut-in speed value of 0.5 m/s (indicated by the green dashed line in Figure 4 (Hagerman and Polagye, 2006; Siagian et al., 2019b), Station 1 exhibits a current capacity of 47.5% that can be harnessed, while Station 2 only has 14.21% available capacity.

Analysis of vertical power density distribution

By employing Equation 1, the power density (W/m^2) was estimated for each depth layer. After

Table 3. Power density estimation (W/m^2) in each depth layer during the measurement period (Maximum and average) based on Equation 1

Depth layer profile no.	Station 1			Station 2		
	Water depth layer (meters)	Power density (W/m^2)		Water depth layer (meters)	Power density (W/m^2)	
		Average	Maximum		Average	Maximum
10	-	-	-	-0.5	15.416	80.700
9	-	-	-	-1	16.481	84.340
8	-1	36.630	240.412	-1.5	18.418	118.053
7	-2	42.185	262.400	-2	19.966	111.254
6	-3	51.529	312.523	-2.5	23.911	129.989
5	-4	62.537	339.816	-3	28.122	235.801
4	-5	66.791	405.620	-3.5	29.705	204.328
3	-6	65.223	436.635	-4	36.630	254.606
2	-7	54.926	447.783	-4.5	31.826	196.112
1	-8	41.032	428.397	-5	22.929	110.700

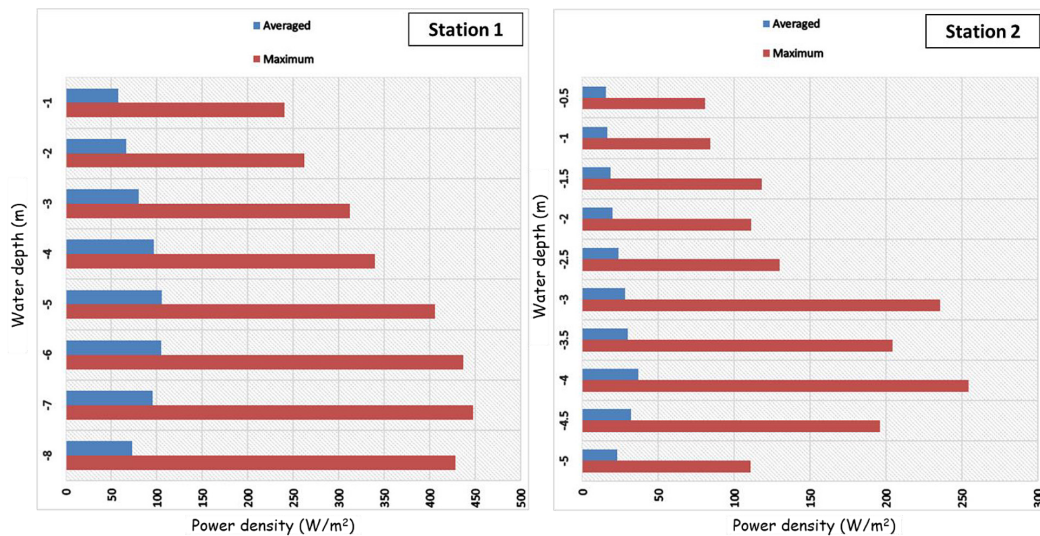


Figure 6. Vertical power density profile from ADCP Stations (Station 1 and Station 2): Average and maximum values for each depth layer

the time variation of velocity is determined, the power density distribution can be readily calculated and averaged in each depth layer (Hagerman and Polagye, 2006), as shown in Table 3. These results were then vertically represented in a graph to visualize the variations in power density at different depths as depicted in Figure 6. These vertical profiles provide insights into the distribution and intensity of power density at different depths within the water column at measuring stations. The results show that the power density generated by tidal currents in each depth layer varies significantly as depth increases. Furthermore, it exhibits a similar and consistent trend from the surface to the bottom at both locations Station 1 and Station 2. At station 1, the average power density in layer 8 is estimated to be 36.63 W/m². As we progress deeper into the layers, specifically layers 7, 6, and 5, the average power density gradually increases, peaking at 66.791 W/m² in layer 4. However, as we progress through layers 3 and 2, the average power density begins to decrease, eventually reaching 41.032 W/m² in layer 1, and the bottom layer. The maximum power density value was observed in layer 2 (-7 m depth), with a power density of 447.783 W/m². Layer 8 (-1 m depth) had the lowest average power density value. At Station 2, the average power density gradually increases as we progress deeper into the layers, specifically layers 9 to 4, peaking at 36.63 W/m² in layer 4. However, as we progress through layer 2, the average power density decreases, eventually reaching 22.929 W/m² in the bottom layer, layer 1. Layer 3 (-4.5 m depth) had the maximum power density value, with a power density of 254.606 W/m², which also had the highest average power density value. The lowest average power density value was found in Layer 10, which was close to the surface (-0.5 m depth).

Station 1 consistently displays significant power density across different depth layers, ranging from 36.63 to 66.791 W/m² throughout the measurement period. Meanwhile, Station 2 features a power density range of 15.416 to 36.63 W/m². The power density estimation results indicate that the highest values observed at Station 1 can be attributed not only to the fact that measurements were taken closest to the spring tide but also because this station is situated in the narrowest and deepest section of the main channel of Khenifiss Lagoon. The heightened velocity in narrower channels contributes to these elevated power density values (Kyojuka and Ogawa, 2006; Garcia

Novo and Kyojuka, 2017). In contrast to Station 1, the lower values observed at Station 2 can be attributed to the fact that measurements were taken closest to the neap tide. Additionally, this station is situated in the upstream and shallower section of the main channel of Khenifiss Lagoon.

Selection of optimal water depth layers for tidal energy extraction

The direct relationship between current velocity and power density emphasizes the importance of vertical profiling in determining the optimal layer for harnessing tidal current energy (Hagerman and Polagye, 2006; Siagian et al., 2019a). According to Neill et al. (2018), the ideal layer for converting current into power density is characterized by a balanced relationship between the average and maximum current velocity values at that depth. It is important to note that not all current speed values can be effectively used to generate electricity. This is why it is crucial to optimize water depth selection and choose turbines with lower cut-in speed values (Hagerman and Polagye, 2006), since current speeds in the lagoon rarely exceed 1 m/s (Lakhdar et al., 2004), and only flow rates exceeding the cut-in speed threshold have sufficient power density capacity for successful electrification.

At Station 1, Layers 2, 3, 4, and 5 (3 to 5 m depth) provide consistent current velocity conditions that are well-suited for power density conversion, with an average power density range during the measurement period in these layers of 54.926 W/m², 62.537 W/m², 66.791 W/m², and 65.223 W/m², respectively. In the same way, at Station 2, Layers 2, 3, 4, 5, and 6 (2.5 to 4.5 m depth) provide the best choice with consistent current velocity conditions suitable for power density conversion, with an average power density range during the measurement period in these layers of 23.911 W/m², 28.122 W/m², 29.705 W/m², 36.630 W/m², and 31.826 W/m², respectively. The selection of these layers for power density generation is based on the observed trend of increasing velocity from the bottom of the water column towards the surface (Bouchkara et al., 2023) as well as the significant potential of tidal energy that can be extracted from these layers. Bottom layers also offer potential for harnessing tidal energy, but with a lower capacity, and are suitable for the deployment of seabed-mounted tidal turbines.

Table 4 offers a comparison between the characteristics of Khenifiss Lagoon and Oualidia

Table 4. Comparison between the characteristics of Khenifiss Lagoon and Oualidia Lagoon

Parameter	Khenifiss Lagoon (This study)	Oualidia Lagoon (Bouchkara et al., 2023)
ADCP deployment depth (meters below LAT)	9 m	6 m
Maximum measured current speed (m/s)	0.965 m/s	1.047 m/s
Averaged measured current speed at different depth layers (m/s)	0.311 m/s to 0.507 m/s	0.229 m/s to 0.580 m/s
Averaged estimated Power density at different depth layers (W/m ²)	15.416 W/m ² to 65.223 W/m ²	0.192 W/m ² to 235.344 W/m ²
Optimal water depth selected for tidal energy extraction (meters Below LAT)	2.5 to 5 meters depth	3 to 4 meters depth

Lagoon (North of Morocco), both situated along the Atlantic coast and sharing nearly identical tidal characteristics but showing distinct morphological differences. The Khenifiss Lagoon, despite being the deepest, exhibits a maximum registered speed of approximately 0.965 m/s. Similarly, the Oualidia Lagoon also records a comparable maximum speed (1.047 m/s). The average measured current speed across various depth layers remains consistent between the two lagoons. However, notable disparities arise in the estimated power density that can be harnessed from these depth layers. In the Khenifiss Lagoon, the average estimated power density spans a range of 15.416 W/m² to 65.223 W/m². Conversely, in the Oualidia Lagoon, this range extends from 0.192 W/m² to a higher value of 235.344 W/m². The optimal water depth for effective tidal energy extraction is suggested to be between 2.5 and 5 meters in the Khenifiss Lagoon, while in the Oualidia Lagoon, it narrows to a range of 3 to 4 meters.

Currently, the majority of tidal energy conversion devices are situated in deep waters (exceeding 30 meters in depth) (Pacheco et al., 2014). Nonetheless, there is significant untapped potential in coastal shallows and estuaries, which have the added benefit of being close to the power grid and having the necessary infrastructure support (Pacheco et al., 2014). Recently, attention has shifted to floating structures for tidal energy conversion, which are typically anchored to the seafloor with chains or cables. This buoyant arrangement enables the positioning of turbines in zones distinguished by peak tidal velocities, consequently improving ease of access for maintenance objectives (Pacheco et al., 2014). In conclusion, the Khenifiss Lagoon's main channel serves as an illustrative instance of a site suitable for the deployment of floating tidal energy conversion devices.

Overall, this study suggests that the main channel of the Khenifiss Lagoon holds the potential as a favorable location for tidal energy extraction.

However, there is a significant knowledge gap regarding the specific dynamics of tidal flows in this area. Therefore, it is imperative to conduct an extensive study to comprehensively assess the tidal energy resources, which should include a long-term evaluation of tidal elevations, spatial and temporal variations in tidal currents, and levels of turbulence.

CONCLUSIONS

Marine current energy holds significant potential to contribute to the future energy supply in the Khenifiss lagoon region, thanks to its appealing qualities, including predictability and its few negative environmental effects. Additionally, turbine installations are more suitable in regions with tidal current fields that reverse along a specific axial direction than in those with currents that have no preferred direction, which is the case of the Khenifiss lagoon main channel, where the current pattern is characterized by two cycles of bidirectional and alternating currents following the semi-diurnal tidal cycles.

The tidal energy resource of the Khenifiss Lagoon's main channel was assessed through field measurements using a bottom-mounted ADCP. The local variability of currents is characterized at two specific sites. The results indicate significant variations in power density generated by tidal currents across different depth layers at both sites (Station 1 and Station 2). At Station 1, Layers 2, 3, 4, and 5 (3 to 5 m depth from the LAT) consistently provide favorable current velocity conditions for power density conversion. The average power density ranges measured during the study period in these layers were 54.926 W/m², 62.537 W/m², 66.791 W/m², and 65.223 W/m², respectively. Similarly, at Station 2, Layers 2, 3, 4, 5, and 6 (2.5 to 4.5 m depth from the LAT) exhibit consistent current velocity conditions suitable for power density

conversion. The average power density ranges measured during the study period in these layers were 23.911 W/m², 28.122 W/m², 29.705 W/m², 36.630 W/m², and 31.826 W/m², respectively. These results highlight that the primary channel of Khenifiss Lagoon is well-suited for the extraction of tidal current energy.

This study establishes a foundation for more detailed tidal current resource assessments and the identification of priority sites, particularly in terms of depth, for future tidal energy development in the lagoon. However, future research should prioritize investigating key aspects to advance tidal current power generation in the lagoon. This includes determining the best system for power generation, taking into account factors such as whether a fixed or floating setup is preferable, and identifying the specific type of system to be used. Furthermore, research should concentrate on ensuring environmental sustainability by mitigating any negative effects on the ecosystem. This entails carefully assessing and mitigating potential environmental impacts to promote the long-term sustainability of tidal current power generation. These key aspects must also include a thorough investigation of the hydrodynamics of the lagoon. Hydrodynamic modeling techniques can be employed to simulate and understand the complex interactions between tidal currents, tides, and other environmental factors, as well as gain insights into the optimal placement and design of tidal current power generation systems. This includes identifying areas with high tidal energy potential, predicting the effects of system deployment on water flow patterns, and assessing potential changes to sediment transport and erosion patterns.

Finally, it should be noted that the water conditions during the measurements, the short duration of the measurements, and the specific locations of the stations may all have a significant impact on the study's results. Long-term measurements are thus required to obtain more accurate and reliable results.

Acknowledgements

The authors would like to express their sincere appreciation to the National Agency of Water and Forests for granting access to the Khenifiss Lagoon. We also extend our gratitude to the local authorities of Akhfennir province for their invaluable support, which made this study possible.

REFERENCES

1. Amimi T., Elbelrhiti K., Adnani M., Elbelrhiti H., Chao J., Oubbih J. 2021. Soil map of Khenifiss lagoon and its surrounding environment. *Arabian Journal of Geosciences*, 14(6), 515.
2. Bahadori A., Nwaoha C., Zendeheboudi S., Zahedi G. 2013. An overview of renewable energy potential and utilisation in Australia. *Renewable and Sustainable Energy Reviews*, 21, 582–589.
3. Beaubrun P.C. 1976. La lagune de Khenifiss: premières observations sur les sédiments et l'hydrologie du milieu. *Bulletin de l'Institut Scientifique de Rabat*, 1, 50–65.
4. Bouchkara M., Siagian H., Erraji Chadid N., Joudar I., Hajjaj C., Benazzouz A., Zourarah B., El Khalidi K. 2023. Potential energy power from tidal current in lagoon system – The case of Oualidia Lagoon, Morocco. *Ecological Engineering & Environmental Technology*, 24(44), 116–127.
5. Boyle G. 1996. *Renewable energy: power for a sustainable future*. Oxford University Press, Oxford.
6. Bryden I.G., Grinsted T., Melville G.T. 2004. Assessing the potential of a simple tidal channel to deliver useful energy. *Applied Ocean Research*, 26(5), 198–204.
7. Dal Ferro B. 2006. Wave and tidal energy: Its emergence and the challenges it faces. *Refocus*, 7(3), 46–48.
8. Dubi A.M. 2007. Tidal power potential in the submerged channels of dar es salaam coastal waters. *Western Indian Ocean Journal of Marine Science*, 5(1), 95104.
9. El Behja H., El M'rini A., Nachite D., Abioui M. 2024a. Assessing the spatiotemporal transformation of a coastal lagoon inlet (1984–2019) using remote sensing and GIS: a study of Khenifiss Lagoon in Southern Morocco. *Environ Earth Sci* 83, 122.
10. El Behja H., El M'rini A, Nachite D, Bouchkara M, El Khalidi K, Zourarah B, 2024b. Hydrodynamic modeling of Khenifiss Coastal Lagoon, Southern Atlantic Coast of Morocco: Implications for sediment infilling. *Thalassas: An International Journal of Marine Sciences* (Accepted for publication)
11. El Behja H, El M'rini A, Nachite D, Bouchkara M, El Khalidi K, Zourarah B, Uddin MG, Abioui M. 2024c. Evaluating coastal lagoon sustainability through the driver-pressure-state-impact-response approach: a study of Khenifiss Lagoon, southern Morocco. *Frontiers in Earth Science*. 12: 1322749.
12. Elbelrhiti H., Andreotti B., Claudin P. 2008. Barchan dune corridors: Field characterization and investigation of control parameters. *Journal of Geophysical Research: Earth Surface*, 113(F2), F02S15.
13. El-Geziry T.M., Couch S.J. 2009. Environmental impact assessment for tidal energy schemes: An

- exemplar case study of the Strait of Messina. *Journal of Marine Engineering and Technology*, 8(1), 39–48.
14. Ellabban O., Abu-Rub H., Blaabjerg F. 2014. Renewable energy resources: Current status, future prospects and their enabling technology. *Renewable and Sustainable Energy Reviews*, 39, 748–764.
 15. Garcia Novo P., Kyojuka Y. 2017. Field measurement and numerical study of tidal current turbulence intensity in the Kobe Strait of the Goto Islands, Nagasaki Prefecture. *Journal of Marine Science and Technology*, 22(2), 335–350.
 16. Ghefiri K., Garrido A.J., Rusu E., Bouallègue S., Haggège J., Garrido I. 2018. Fuzzy supervision based-pitch angle control of a tidal stream generator for a disturbed tidal input. *Energies*, 11(11), 2989.
 17. González-Gorbeña E., Rosman P.C.C., Qassim R.Y. 2015. Assessment of the tidal current energy resource in São Marcos Bay, Brazil. *Journal of Ocean Engineering and Marine Energy*, 1(4), 421–433.
 18. Guerra M., Cienfuegos R., Thomson J., Suarez L. 2017. Tidal energy resource characterization in Chacao Channel, Chile. *International Journal of Marine Energy*, 20, 1–16.
 19. Hagerman G., Polagye B. 2006. Methodology for estimating tidal current energy resources and power production by tidal in-stream energy conversion (TISEC) devices. Technical Report, Electric Power Research Institute, Palo Alto.
 20. Hwang I.S., Lee Y.H., Kim S.J. 2009. Optimization of cycloidal water turbine and the performance improvement by individual blade control. *Applied Energy*, 86(9), 1532–1540.
 21. IEA 2019. Energy Policies beyond IEA Countries: Morocco 2019. International Energy Agency, Paris.
 22. Kyojuka Y., Ogawa K. 2006. Tidal Current Power Generation Making Use of a Bridge Pier. In: *Proceedings of the OCEANS 2006—Asia Pacific*, Singapore, 16–19 May 2006, 1–8.
 23. Lakhdar Idrissi J., Orbi A., Zidane F., Hilmi K., Sarf F., Massik Z., Makaoui A. 2004. Organization and functioning of a Moroccan ecosystem: Khnifiss lagoon. *Journal of Water Science*, 17(4), 447–462.
 24. Mirari S., Aoulad-Sidi-Mhend A., Benmlih A. 2020. Geosites for geotourism, geoheritage, and geoconservation of the khnefiss national park, southern Morocco. *Sustainability*, 12(17), 7109.
 25. Multon B. 2013. *Marine Renewable Energy Handbook*. Wiley, New York.
 26. Musa S.D., Zhonghua T., Ibrahim A.O., Habib M., 2018. China's energy status: A critical look at fossils and renewable options. *Renewable and Sustainable Energy Reviews*, 81(2), 2281–2290.
 27. Neill S.P., Angeloudis A., Robins P.E., Walkington I., Ward S.L., Masters I., Lewis M.J., Piano M., Avdis A., Piggott M.D., Aggidis G., Evans P., Adcock T.A.A., Židonis A., Ahmadian R., Falconer R. 2018. Tidal range energy resource and optimization – Past perspectives and future challenges. *Renewable Energy*, 127, 763–778.
 28. Neill S. P., Haas K. A., Thiébot J., Yang Z. 2021. A review of tidal energy – Resource, feedbacks, and environmental interactions. In *Journal of Renewable and Sustainable Energy*.
 29. Pacheco A., Ferreira Ó., Carballo R., Iglesias G. 2014. Evaluation of the production of tidal stream energy in an inlet channel by coupling field data and numerical modelling. *Energy*, 71, 104–117.
 30. Pu X., Shi J.Z., Hu G.D. 2017. The effect of stratification on the vertical structure of the tidal ellipse in the Changjiang River estuary, China. *Journal of Hydro-Environment Research*, 15, 75–94.
 31. Rourke F. O., Boyle F., Reynolds A. 2010. Marine current energy devices: Current status and possible future applications in Ireland. *Renewable and Sustainable Energy Reviews*, 14(3), 1026–1036.
 32. Rourke F. O., Boyle F., Reynolds A. 2009. Renewable energy resources and technologies applicable to Ireland. *Renewable and Sustainable Energy Reviews*, 13(8), 1975–1984.
 33. Siagian H., Ismanto A., Putra T. W. L., Pranata 2021. Stratification on the Vertical Structure of the Tidal Ellipse and Power Density Estimation in the Larak Strait, East Flores Based on ADCP Measurement Data. In: *IOP Conference Series: Earth and Environmental Science*, Indonesia.
 34. Siagian H., Sugianto D.N., Kunarso 2019a. Current Velocity Impacts from Interaction of Semidiurnal and Diurnal Tidal Constituents for Tidal Stream Energy in East Flores. In: *IOP Conference Series: Earth and Environmental Science*, Indonesia.
 35. Siagian H., Sugianto D. N., Kunarso, Pranata A.S. 2019b. Estimation of Potential Energy Generated from Tidal Stream in Different Depth Layer at East Flores Waters Measured by ADCP. *IOP Conference Series: Earth and Environmental Science*, Indonesia.
 36. Vanegas Cantarero M.M. 2020. Of renewable energy, energy democracy, and sustainable development: A roadmap to accelerate the energy transition in developing countries. *Energy Research and Social Science*, 70, 101716.
 37. Wang Z., Carriveau R., Ting D. S. K., Xiong W., Wang Z. 2019. A review of marine renewable energy storage. *International Journal of Energy Research*, 43(12), 6108–6150.
 38. Wei Z., Fang G., Susanto R.D., Adi T.R., Fan B., Setiawan A., Li S., Wang Y., Gao X. 2016. Tidal elevation, current, and energy flux in the area between the South China Sea and Java Sea. *Ocean Science*, 12(2), 517–531.
 39. Zabihian F., Fung A.S. 2011. Review of marine renewable energies: Case study of Iran. *Renewable and Sustainable Energy Reviews* 15(5), 2461–2474.